https://eprints.gla.ac.uk/290017/

Deposited on: 26 January 2023

A synergistic {Cu$_2$-W$_{12}$O$_{40}$} catalyst with high conversion for homo-coupling of terminal alkynes

Zhan-Guo Jiang‡[a], Hui-Min Zeng‡[a], Xiangyu Zhang[a], Yuan Tan[b], You-Zhao Lan[a], Yu Wang[a], De-Liang Long*[c], Leroy Cronin*[c] and Cai-Hong Zhan*[a]

[a]*Key Laboratory of the Ministry of Education for Advanced Catalysis Material, Institute of Physical Chemistry, College of Chemistry and Life Sciences, Zhejiang Normal, University, No. 688, Yingbin Avenue, Jinhua, Zhejiang 321004, China. E-mail: chzhan@zjnu.cn*
[b]*Hangzhou Institute of Advanced Studies, Zhejiang Normal University, Hangzhou 311231, China*
[c]*School of Chemistry, The University of Glasgow, Glasgow G12 8QQ, UK. E-mail: Deliang.Long@glasgow.ac.uk; Lee.Cronin@glasgow.ac.uk*

‡ These authors contributed equally to this work.

Abstract

By the strategy of replacing the H$_2$O ligands in the "paddle wheel" shaped copper dimer Cu$_2$(OAc)$_4$(H$_2$O)$_2$ with polyoxometalate (POM) [H$_2$W$_{12}$O$_{40}$]$^{6-}$ {W$_{12}$O$_{40}$} pro-ligands, a novel nano porous 2D network {[Cu$_2$(OAc)$_4$]$_2$(W$_{12}$O$_{40}$)}$_n$ was obtained. The POM – copper centered redox reactions and stability of the compound were studied by cyclic voltammetry. Furthermore, the compound was found to be a super-efficient homogeneous catalyst (almost 100% conversion) in homo-coupling of terminal alkynes compared with its components and physical mixture under mild conditions with low amounts. The *in situ* Diffuse Reflectance Infrared Fourier Transform Spectroscopy (DRIFTS) results clearly show the changes of alkyne substances in the catalytic process and the X-ray photoelectron spectroscopy (XPS) results reveal the electron transfer from {W$_{12}$O$_{40}$} to Cu(II) to promote the C–H activation step during the homo-coupling of terminal alkynes. The synergistic Cu(II)-POM catalytic mechanism was proposed.

Introduction

In recent years, copper catalysts have been widely used in nucleophilic addition, ring addition, oxidation and many other reactions.[1–5] Compared with precious metals such as Pd, Au, Rh and Ni, Cu and its complexes are characterized by their versatility, low cost, low toxicity and high efficiency. As is well known, the discovery of the Ullmann coupling reaction provides an important method for the construction of carbon–carbon bonds and carbon–heterogeneous bonds.[6] However, traditional Ulmann coupling reactions are harsh and require high temperatures, and excessive copper powder catalysts, and the yield is not high.[7,8] In 1998, the Ma group found that copper catalysts with ligand participation could promote the Ulmann coupling reaction.[9] In recent years, the ligand-promoted copper catalytic coupling reaction has made great progress, and the new catalytic system is more green, economical and efficient than before.[10–14]

Copper(II) acetate monohydrate, one of the ligand-promoted copper catalysts, adopting a "paddle-wheel" structure, is often used as an oxidant in organic synthesis. For example, Cu$_2$(OAc)$_4$(H$_2$O)$_2$ can catalyze the coupling of two terminal alkynes, the product of which is 1,3-diacetylene, Cu$_2$(OAc)$_4$ + 2

RC≡CH → 2 CuOAc + RC≡C–C≡CR + 2 HOAc.[15] For this dimeric unit structure, other small molecular ligands like dioxanes, pyridines, and aniline can all replace the water molecules in the above dimer,[16,17] however, the inorganic nano-sized polyoxometalates (POMs) as molecular ligands have not been reported yet.

POMs are a remarkable class of discrete anionic metal oxide clusters, which can maintain the structure unchanged when they go through redox reactions. POMs are applicable in many fields such as photochemistry, catalysis,[18–20] magnetism, molecular electronics, medicine and materials science.[21–24] Actually, POMs offer huge potentialities as subcomponents in constructing hybrid materials owing to their wide range of compositions, structures and multiple linking points on the surface of the clusters.[25] Mizuno *et al.* reported that a monomeric γ-Keggin silicotungstate with a dicopper core that is bridged by two μ-1,1-azido ligands catalyzes the homocoupling reactions of terminal alkynes.[23] Assembly of functional materials from simple nano-sized building blocks usually involves complicated self-organization processes and thus is a long-standing challenge. Herein, by the strategy of replacing water pro-ligands on the apical coordinate sites of the "paddle wheel" shaped copper dimer $Cu_2(OAc)_4(H_2O)_2$ with Keggin type POM $[H_2W_{12}O_{40}]^{6-}$ $\{W_{12}O_{40}\}$ pro-ligands, a nanoporous 2D network of composition $\{[Cu_2(OAc)_4]_2(W_{12}O_{40})\}_n$ **1** was obtained.

1 was found to be an efficient catalyst in the homo-coupling of terminal alkynes and can easily be recovered after the reaction and reused with the retention of its high catalytic performance. The synergistic binary Cu(II)-POM catalytic system can be used for the formation of C–C bonds under mild reactions, without suffering from the usage of high amounts of catalyst and TEMPO ((2,2,6,6-tetramethylpiperidin-1-yl)oxidanyl), and some expensive bases such as DABCO (1,4-diazabicyclo[2.2.2]octane) reported in the literature.[24] This protocol can be considered as an alternative to palladium and does not require the use of expensive and/or air-sensitive phosphine ligands that are often required in the palladium chemistry.[25] **1** was also comparable to well-established Cu-based catalysis of Glaser or Hay couplings.[15] (see Table S2†) What's more, this work provides new ideas for the structural design, synthesis and application of heterometallic POM-based functional materials, and also sets up a model for the effective electron transfer in catalytic applications.

Results and discussion

Crystal structure of 1

The porous 2D network of **1** is built from "paddle wheel" shaped copper dimers $Cu_2(OAc)_4$ and Keggin type POM $\{W_{12}O_{40}\}$ pro-ligands. From single-crystal X-ray diffraction data, in $Cu_2(OAc)_4(H_2O)_2$, one oxygen atom in each acetate is bound to one copper atom, and the bond length of Cu–O is 195.4 pm on average (see Fig. 1a). Two water molecular ligands occupy the apical coordinate sites and the bond length of Cu–O are around 217.2 pm. The distance between two copper atoms is 261.5 pm, close to the Cu–Cu distance (255 pm) in metal copper. In **1**, the apical coordinate sites of the copper dimer are occupied by $\{W_{12}O_{40}\}$ Keggin type POM ligands (see Fig. 1b).
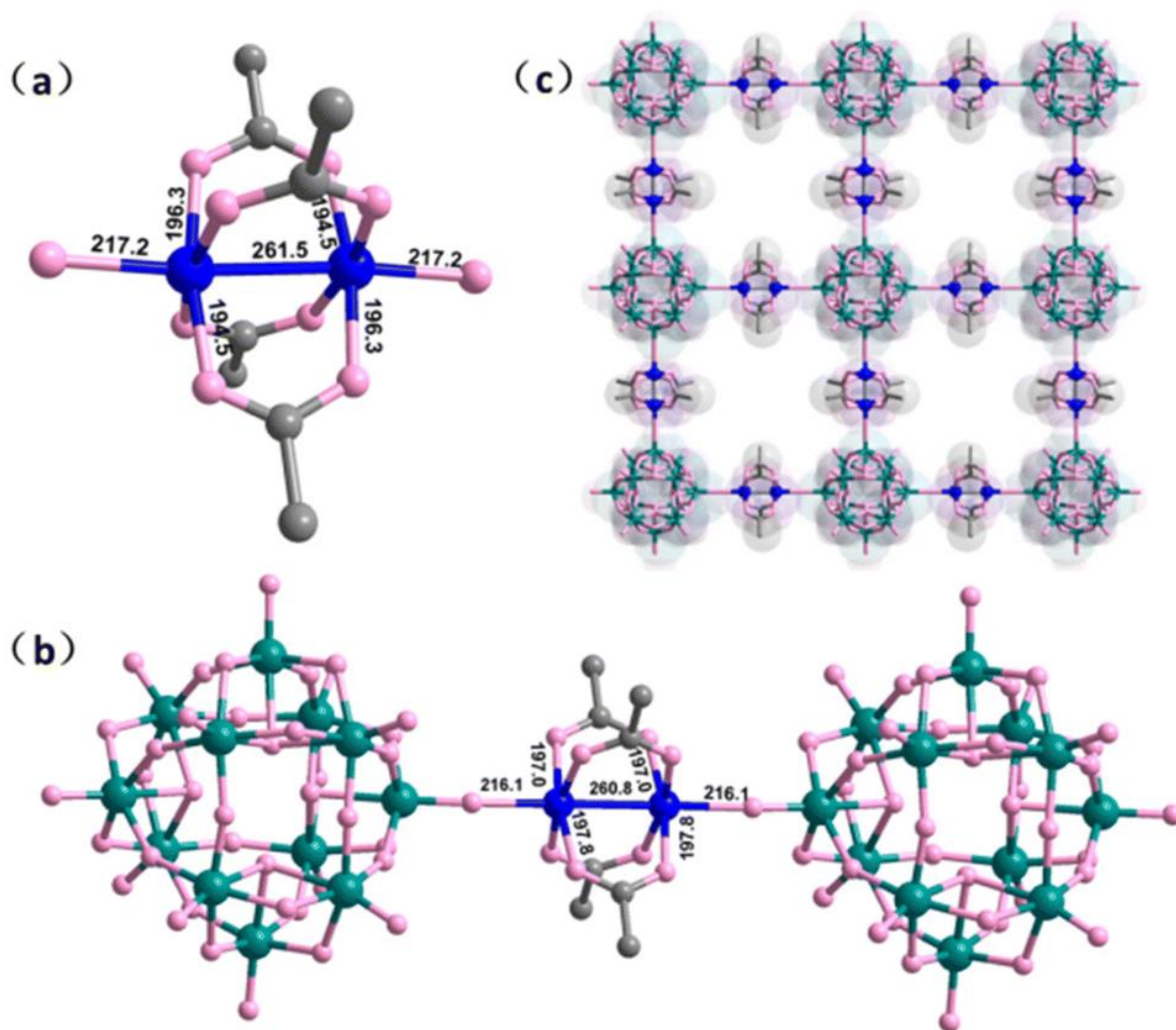
Fig. 1 - Representation of the structure for Cu₂(OAc)₄(H₂O)₂ (a); a dumbbell species Cu₂(OAc)₄(POM)₂ shows local connection between Cu₂(OAc)₄ and {W₁₂O₄₀} (b); and one layer of porous 2D network in **1** *(c). Cu, W, O and C are shown in blue, teal, rose and grey.*

Compared with the "paddle wheel" shaped copper acetate molecule, the distance of two copper ions in **1** is slightly shortened from 261.5 to 260.8 pm. The bond length of Cu–O (acetate) is lengthened to 197.4 pm on average, which means that the replacement of apical site H_2O in "paddle wheel" shaped copper dimers with the Keggin type POM pro-ligand will weaken the bond strength between copper cations and acetate anions. The bond length of Cu–O (POM) is shortened to 216.1 pm, which means the POM pro-ligand has a stronger interaction with copper than the water ligand. Furthermore, we calculated the change in the total energy (ΔE) of the reaction $Cu_2(OAc)_4(H_2O)_2$ + 2(POM) → $Cu_2(OAc)_4(POM)_2$ + 2(H_2O) using density functional theory. The calculations were based on the B3LYP hybrid functional with the LanL2DZ basis set as implemented in the Gaussian03 program. The experimental geometries were used for calculations. The calculated ΔE is −149.6 kcal mol^{-1}, which indicates that this reaction should be energetically feasible for POM coordination with a dumbbell species $Cu_2(OAc)_4(POM)_2$ (Fig. 1b) as an example. In **1**, each POM {W₁₂O₄₀} cluster links four copper dimers $Cu_2(OAc)_4$ *via* four W=O terminal oxo from the opposite belt positions in the crystallographic *a* and *b* directions (see Fig. 1c). Thus {W₁₂O₄₀} clusters as 4-connected linkers connect four "paddle wheel" shaped copper dimers to form a (4, 4) 2D porous network with a pore

size of 11.3 Å × 11.3 Å. It is worth noting that the stacking mode of the structure is the AB model in order to reach dense packing (Fig. S1†), so the final pore size is 8.2 Å × 8.2 Å.

Cyclic voltammetry

One of the extraordinary properties of POMs is their ability to undergo multielectron redox reactions with almost no change in the structure. In order to investigate the redox properties of the "paddle wheel" shaped dimer copper linked by POMs, cyclic voltammetry (CV) experiments were conducted. The CV curve of a 0.1 M aqueous solution of **1** shows three reversible peaks at −0.87, −0.73, and −0.24 V, corresponding to the SCE (Fig. 2a). The first reduction wave, peaking at −0.24 V, can be assigned to the reduction of the Cu(II) centres. In addition to the Cu-centred processes, two typical reversible wave couples ($E_{1/2}$ = −0.73 V, −0.87, V) associated with redox processes for W(VI) based-species can also be observed in the cathodic region of the voltammogram. Additionally, replacing the H_2O ligands of the "paddle wheel" shaped dimer coppers with the POM $\{W_{12}O_{40}\}$ pro-ligands has a beneficial effect on the stabilization of the POM and copper dimer, as $Cu_2(OAc)_4(H_2O)_2$ causes irreversible redox processes under equivalent experimental conditions (Fig. 2b). The CV curve shows almost no change in the redox peaks after 3 cycles, which demonstrates that the POM is still bonded to the copper dimer in the solution. The stabilization induced by complexion in aqueous solution is attributed to both electronic perturbations, as observed in the CV experiments, and steric protection from the POM.
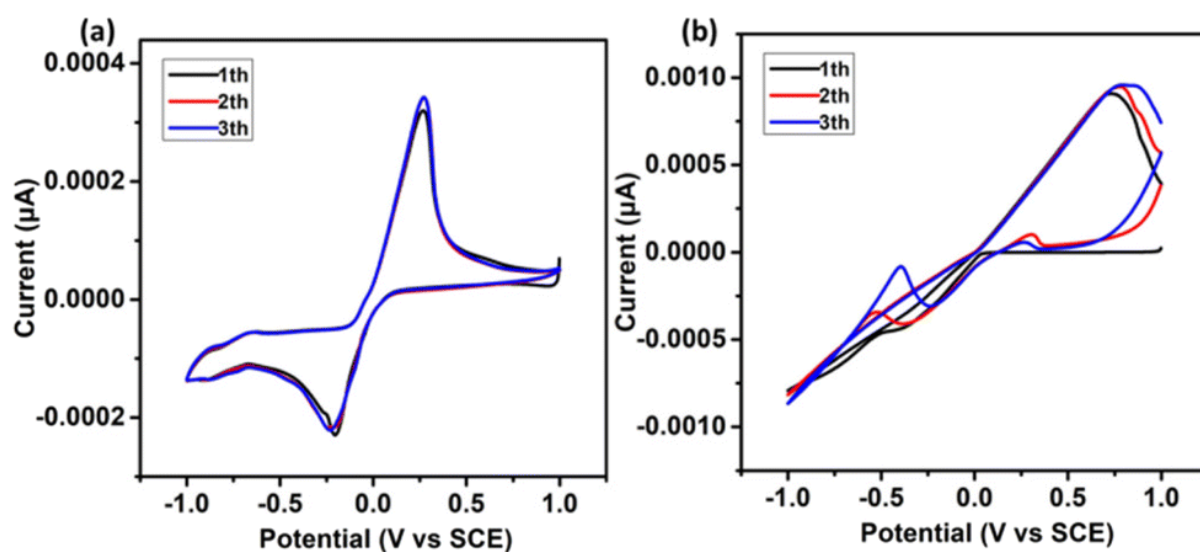

Fig. 2 - Cyclic voltammograms (298 K, scan rate 500 mV s⁻¹) of 1 (a) and Cu₂(OAc)₄(H₂O)₂ (b) for 3 cycles.

Catalytic activity of 1 in the homo-coupling of phenylacetylene

Alkynes are one of the most important building blocks in organic synthesis, industry and many natural compounds. Hence, scientists have paid much attention to the homo-coupling reaction of terminal alkynes. The Cu(II)-POM composite **1** was tested in the catalyzed homo-coupling reaction of terminal phenylacetylenes under atmospheric conditions (Scheme 1). The reaction was done under various reaction conditions (THF and DMF as solvents, KOH as the base, temperature, concentration and time) (see Table 1). When DMF was used as the solvent, the corresponding coupling product was acquired in moderate yield (45%; Table 1, entry 1). A higher reaction temperature, a larger amount of **1** or a prolonged reaction time were required to get satisfactory results (Table 1, entries

2–8). The coupling of phenylacetylene afforded almost 100% conversion in 3.5 h at 100 °C or in 4.5 h at 90 °C with a catalyst amount of 3 mol% (Table 1, entries 4 and 8). The comparison between the activities of $\{PW_{12}O_{40}\}$ (as the Keggin type POM $\{PW_{12}O_{40}\}$ is much more stable than $\{W_{12}O_{40}\}$, in the comparison experiment, $\{PW_{12}O_{40}\}$ was utilized), $Cu_2(OAc)_4(H_2O)_2$ and $Cu_2(OAc)_4(H_2O)_2 + \{PW_{12}O_{40}\}$ for phenylacetylene homo-coupling reactions has also been performed and is listed in Table 1 (entries 9–11), which show that **1** has much better activity for homo-coupling reactions than its components separately or their physical mixture. The chemical doping of the POM ($\{W_{12}O_{40}\}$) to dimer copper centers largely promotes homo-coupling reactions. The recycling experiments showed that even in the third recycling process, the coupling of phenylacetylene also afforded almost 100% conversion (Table 1, entries 12–14). Besides the homo-coupling product of phenylacetylene, as shown in Table 2, the aromatic (with various substituents on the ring including electron-donating alkoxy, electron-accepting fluoro) and aliphatic alkynes can also undergo homo-coupling reactions smoothly (see S10 in the ESI† for details). The effect of steric hindrance of terminal alkynes on the $\{POM_2\text{-}Cu_2\}$ catalytic center was studied using DFT calculations. As shown in Fig. S32,† the aromatic rings of the substrates are inclined close to the catalyst and the substituents (−F and −OMe) are far away from the POM to avoid steric hindrance). However, a poor result was obtained when THF was employed as a solvent even with a base as an additive (Table 1, entries 15, 16 and Fig. S33†), which suggested that DMF could play dual roles as both a base and a reducing reagent in the reaction.
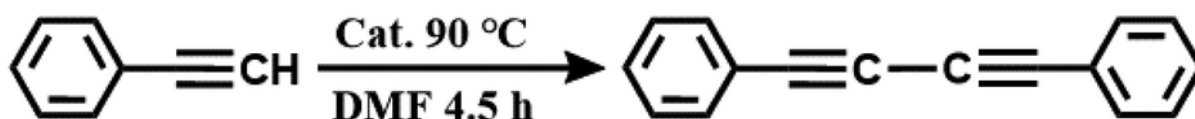
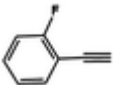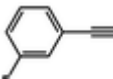Scheme 1 - Homo-coupling of phenylacetylene by **1** as a catalyst.

Table 1 - Catalytic activity of **1** in the homo-coupling of phenylacetylene under various reaction conditions

Entry	Catalyst	Solvent	T (°C)	Catalyst (mol%)	T (h)	Conversion (%)
1	**1**	DMF	60	3	4.5	45
2	**1**	DMF	70	3	4.5	62
3	**1**	DMF	80	3	4.5	86
4	**1**	DMF	90	3	4.5	>99.5

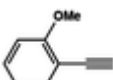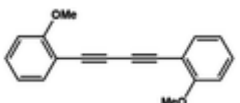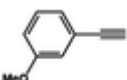| Entry	Catalyst	Solvent	T (°C)	Catalyst (mol%)	T (h)	Conversion (%)
5	**1**	DMF	90	1	4.5	18
6	**1**	DMF	90	2	4.5	48
7	**1**	DMF	90	3	3.5	79
8	**1**	DMF	100	3	3.5	>99.5
9	$Cu_2(OAc)_4(H_2O)_2$	DMF	90	3	4.5	31
10	$\{PW_{12}O_{40}\}$	DMF	90	3	4.5	0
11	$Cu_2(OAc)_4(H_2O)_2$ + $\{PW_{12}O_{40}\}$	DMF	90	3	4.5	56
12[a]	**1** 1th	DMF	90	3	4.5	>99.5
13[a]	**1** 2th	DMF	90	3	4.5	>99.5
14[a]	**1** 3th	DMF	90	3	4.5	>99.5
15	**1**	THF	90	3	4.5	25
16[b]	**1**	THF	90	3	4.5	70

a **The catalyst can easily be recovered after the reaction and recovery in air by the addition of an excess of diethyl ether (precipitation method). These experiments involved the use of a recycled catalyst: 1st recycling (entry 12), 2nd recycling (entry 13), and 3rd recycling (entry 14) processes. The reaction was carried out under the same conditions as in entry 4.** *b* **KOH (0.12 g) is added as a base and stirred under the reaction conditions. Note: the catalyst in THF was largely decomposed after the reaction and formed by-products.**

*Table 2 - Catalytic activity of **1** in the homo-coupling of alkyne derivatives*

Entry	Substrates	Product	Conversion(%)
1			>99.5
2			>99.5
3			>99.5
4			>99.5
5			>99.5
6	n-C₇H₁₅——≡	n-C₇H₁₅————n-C₇H₁₅	>99.5

Reactions were carried out under the same conditions as in entry 4 in Table 1.

The mechanistic research of Cu-POM catalyzed coupling reactions is challenging but helpful for designing new catalytic systems. We proposed a possible mechanism in the coupling reactions catalyzed by the Cu-POM based on the reported model involving the Cu(II)–Cu(I) synergistic procedure.[26,27] (Scheme 2).
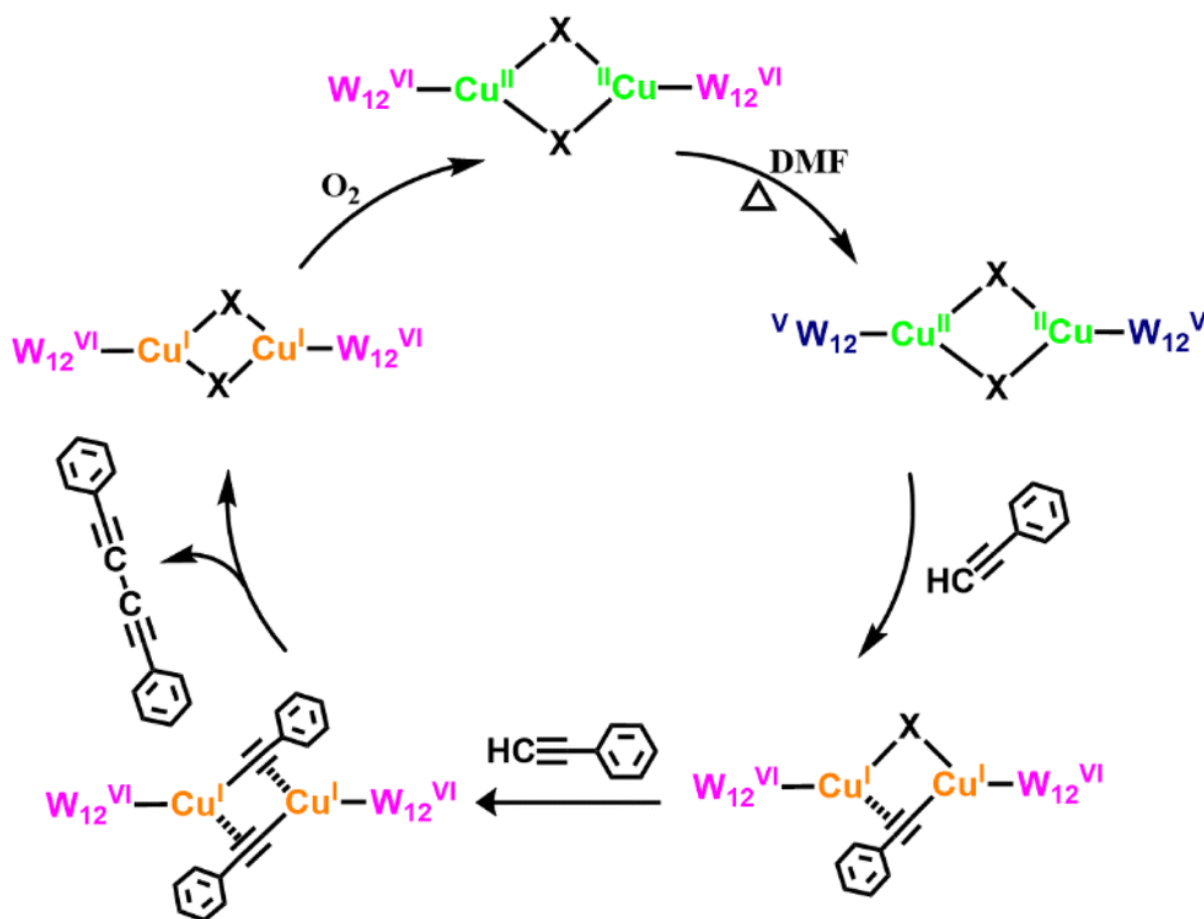
*Scheme 2 - Plausible reaction mechanism of the homo-coupling of phenylacetylene by **1**.*

As the 2D framework of **1** dissolved in solution is fractured as pieces of multiple {Cu$_2$} dimers and {W$_{12}$O$_{40}$}, most possibly with {W$_{12}$O$_{40}$} as terminals along sides, which is confirmed using DFT calculations and CV experiments. The composition of the catalyst after the catalytic reaction was characterized by high-resolution mass spectrometry. As shown in Fig. S31,† the negative-ion ESI-MS shows several groups of signals, corresponding to −3 −4 and −1 species, in the *m/z* range of 1800–3000. After carefully matching experimental mass spectra with calculated isotope distributions, each envelope containing different species can be identified. The envelope in the *m/z* range of 1800–2100 is −3 charged species, and the major mass peaks are identified as follows: [(H$_2$W$_{12}$O$_{40}$)$_2$Cu(H$_2$O)$_4$H$_7$]$^{3-}$ and [(H$_2$W$_{12}$O$_{40}$)$_2$Cu$_2$(CH$_3$COO)$_4$(H Na)$_9$]$^{3-}$. The envelope in the *m/z* range of 2200–2400 is −4 charged species, and the major mass peaks are identified as follows: [(H$_2$W$_{12}$O$_{40}$)$_3$Cu$_2$(H$_2$O)$_8$H$_{14}$]$^{4-}$ [(H$_2$W$_{12}$O$_{40}$)$_3$Cu$_2$(CH$_3$COO)$_4$Cu(H$_2$O)$_4$H$_9$Na$_3$]$^{4-}$ and [(H$_2$W$_{12}$O$_{40}$)$_3$Cu$_4$(CH$_3$COO)$_8$H$_9$Na$_5$]$^{4-}$. The envelope in the *m/z* range of 2800–3000 is −1 charged species, and the major mass peaks are identified as follows: [(H$_2$W$_{12}$O$_{40}$)H$_1$Na$_4$]$^-$. The results show that the catalyst was decomposed into several components, including single copper units and copper dimer units. The real catalytic center should be copper dimer units of {POM$_2$-Cu$_2$} based on the reported model involving the Cu(II)–Cu(I) synergistic cooperation procedure.[26,27] The dumbbell species Cu$_2$(OAc)$_4$(POM)$_2$ (Fig. 1b) was taken as a representative model. It is well known that POMs tend to become heteropoly blue under reducing conditions. Firstly, the DMF reduces partial W(VI) in the POM to W(V) at 90 °C (step 1 in Scheme 2), which can be proved by the observation of dark blue solution and XPS of W (see the subsequent analysis), and then W(V) in the POM reduces Cu(II) to

Cu(I) (including a little Cu(0)) and causes acetate ligands to be partially disconnected (step 2 in Scheme 2); simultaneously two phenylacetylene molecules coordinate to Cu(I) as Cu(I) has a stronger interaction with phenylacetylene than Cu(II).[23,27] By this step, the inactive C–H bond is activated, and this step is considered as the RDS according to previous literature studies.[26] The subsequent inner sphere electron transfer breaks the Cu–C bonds and forms C–C bonds. The attack of acetate back to the Cu center releases the oxidative homo-coupling product (step 4 in Scheme 2). And finally Cu(I) is oxidized back to Cu(II) by O_2 in air (step 5 in Scheme 2), in which the first cycle ends and the second cycle starts. Hence, as against other catalysts mentioned in the literature,[7,8,24] we have not used any additives in this reaction. The POM as the assistant catalyst promotes the homo-coupling of phenylacetylene. During this reaction, the color of the dissolved catalyst in DMF changes to dark blue (step 1 in Scheme 2). When the reaction goes on for a longer time, the color of the catalyst turns greenish yellow, which shows the generation of the Cu(I) complex (step 2 in Scheme 2). After the reaction completes and remains in air, the color recovers to light blue, which proves the recovery of the Cu(II) – POM (W(VI)) catalyst (step 5 in Scheme 2). It should be noted that the dual role of the POM is in coordination with the copper dimer as a ligand to stabilize the structure and in assisting the reduction of Cu(II) to Cu(I), which facilitates the coordination of acetylene with Cu(I) to promote C–H activation.

IR spectroscopy has been widely used and provided meaningful structural information on reaction intermediates in various reactions. Herein, *in situ* DRIFTS was employed to detect the changes in alkyne substances (see Fig. 3). When phenylacetylene was introduced into the DMF solution of the sample cell, a typical peak at 3306 cm^{-1} (stretching vibration of the hydrocarbon bonds on the alkyne) appeared, which disappeared when the temperature rose to 60 °C, and a new peak at 1250 cm^{-1} (C–C single bond skeleton vibration of the homo-coupling of terminal alkyne) appeared.[28] It should be noticed that *in situ* DRIFTS, only 10 μL of DMF and 10 μL of phenylacetylene were added into the sample in order to avoid corrosion to the sample cell. The catalytic reaction was complete in 40 min. The peak of the intermediate Cu(I)-phenylacetylene showed up at 815 cm^{-1}.[27] (Fig. S30†) Meanwhile the cumulative double bond region (2200 cm^{-1}–2600 cm^{-1}) suggested the formation of the coupling product. The peak at 1598 cm^{-1} (the skeleton vibration of the benzene ring) becomes more obvious. It is also worth noting that due to the large electric dipole moment of carbonyl, generally, the absorption is very strong and often becomes the first strong peak (1675 cm^{-1}) in the IR spectrum. The *in situ* DRIFTS spectra here clearly show the changes of alkyne substances in the catalytic reaction and support our putative mechanism.
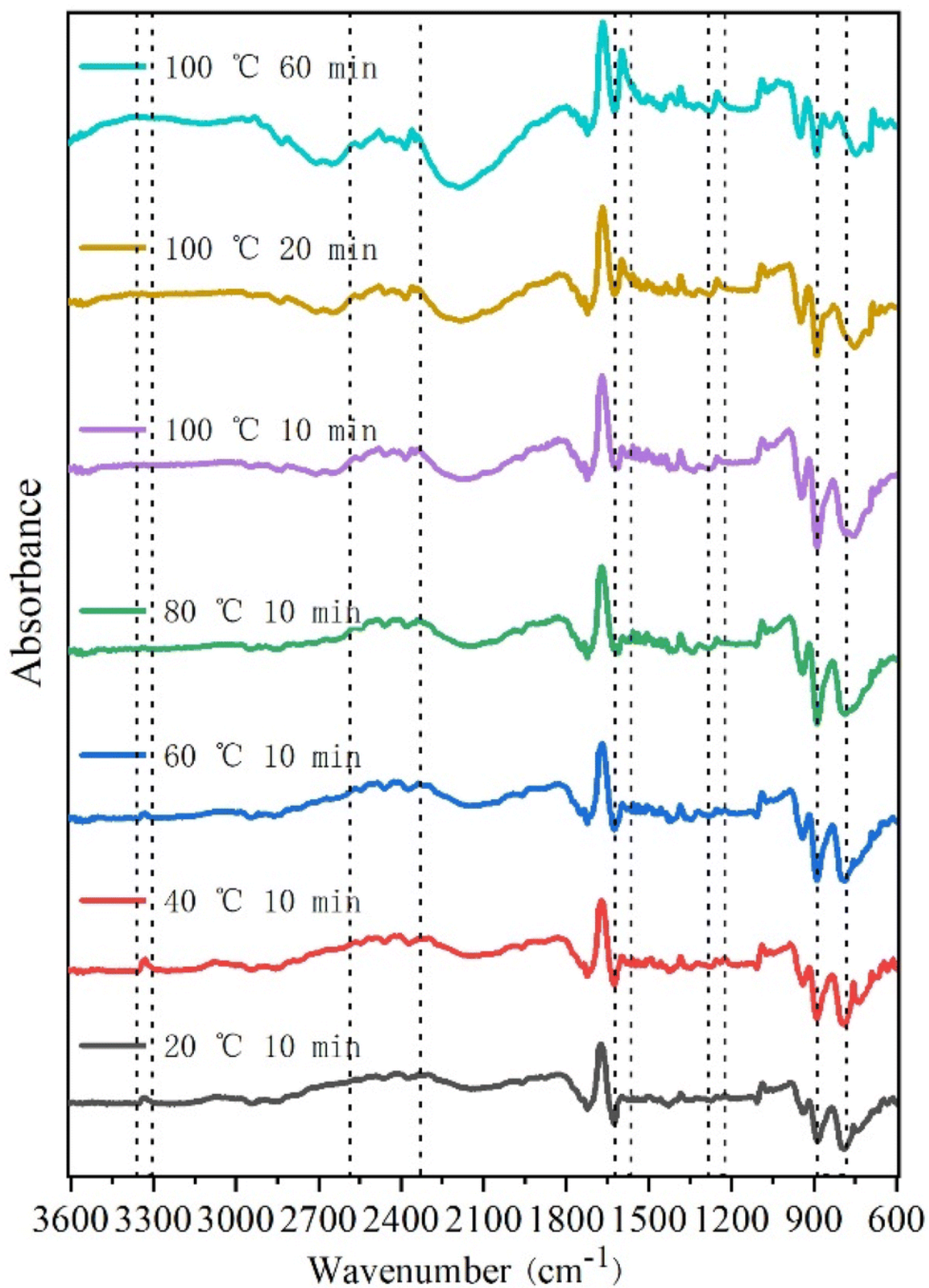
Fig. 3 - In situ DRIFTS of homo-coupling of phenylacetylene by 1.

In order to further investigate the surface states of **1** during the oxidization and reduction processes in the homo-coupling reactions in air, X-ray photoelectron spectroscopy (XPS) was performed and the results are shown in Fig. 4. After the reaction was conducted for 2 h, the greenish yellow catalyst was collected and measured by XPS. The XPS studies exhibit that the peaks of W $4f_{7/2}$ W $4f_{5/2}$ (36.3 and 38.4 eV) indicate the formation of W/O bonding and W(VI) (see Fig. 3a), which means that the reduced W(V) is oxidized to W(VI) during the reduction of Cu(II) (step 2 in Scheme 2).[29,30] The reduction of Cu(II) would get Cu(I) or Cu(0). Since the binding energies of Cu 2p for the Cu(I) and Cu(0) are very close, the Auger electron spectroscopy (AES) peaks of Cu LMM were measured to distinguish Cu(I) from Cu(0), as shown in Fig. 3b. Two different LMM Auger kinetic energies at ~917 and ~920 eV, corresponding to Cu(I) and Cu(0) (2.4 : 1), respectively.[31] When the coupling reaction was completed totally in air, the dark blue catalyst was collected and measured by XPS. The XPS data exhibit that the peaks of W $4f_{7/2}$ W $4f_{5/2}$ (35.7 and 37.8 eV) move to a lower kinetic energy indicating the formation of W/O bonding and W(V) (see Fig. 3c). The Cu 2p XPS spectra show peaks corresponding to Cu $2p_{3/2}$ spin–orbit (~934 eV), Cu $2p_{1/2}$ spin–orbit (~954 eV) and its satellite peaks (~944 and 963 eV), which is consistent with the presence of Cu(II) (see Fig. 3d). It is proved that the oxidation process of Cu(I) and Cu(0) back to Cu(II) by O_2 in air and the reduction of W(VI) to W(V) in the POM at 90 °C in DMF (steps 5 and 1 in the next cycle in Scheme 2).
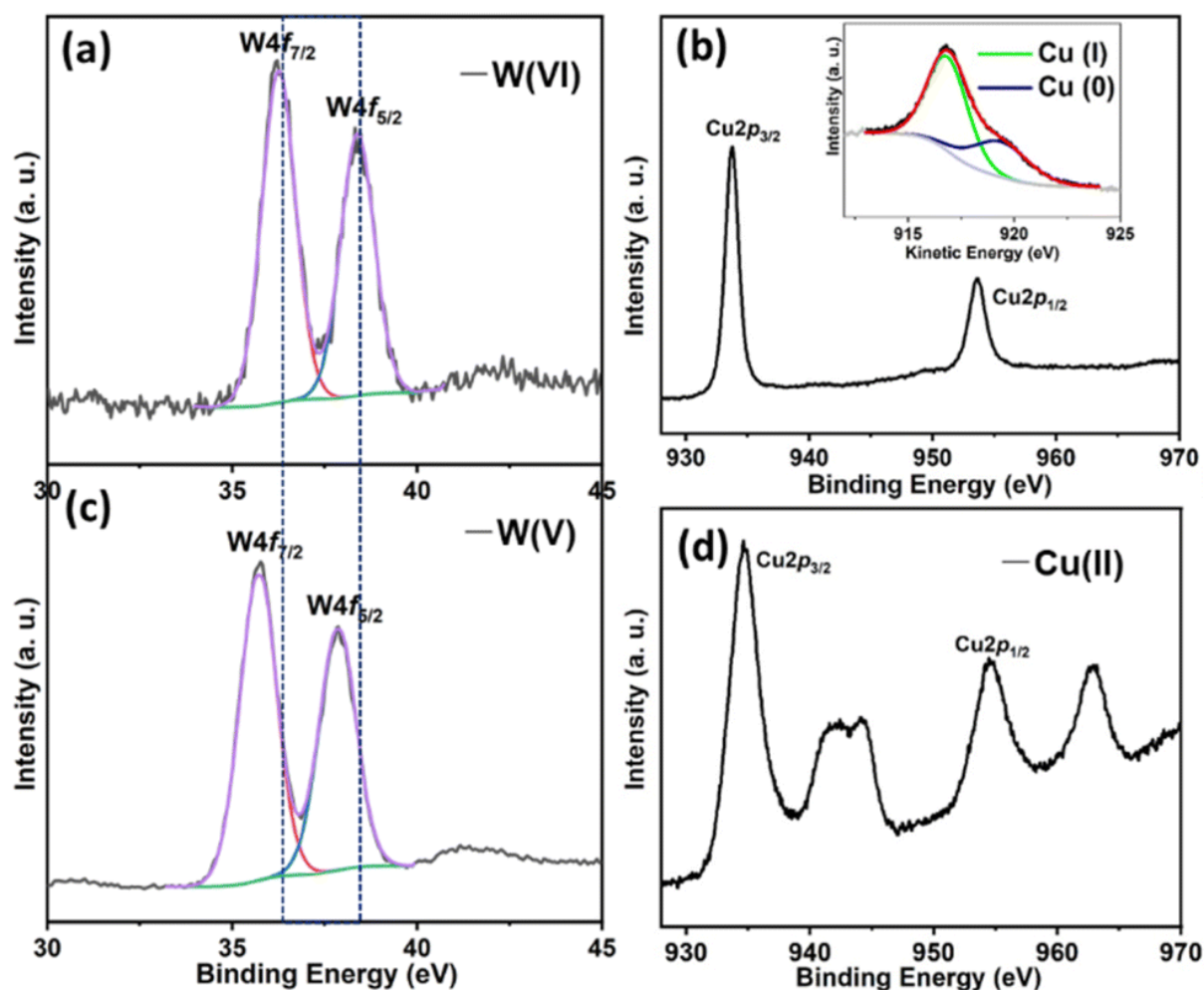

Fig. 1 - XPS of W4f (a and c) and Cu 2p (b and d).

Conclusions

In summary, the reaction of "paddle wheel" shaped $Cu_2(OAc)_4(H_2O)_2$ with the POM $\{W_{12}O_{40}\}$ pro-ligand results in a nano-sized porous 2D network. Compared with other synthetic methods, the synthesis of the title compound has better controllability for the target products and better reflects the ideology of the design. The redox reactions and stability of the easily handled $\{Cu_2\text{-}W_{12}O_{40}\}$ composite were studied by cyclic voltammetry. Furthermore, a low amount of the catalyst in safe media under mild conditions was first employed to obtain homo-coupling products in almost 100% yields, in which the POM functions as the assistant catalyst to effectively transfer electrons to promote the C–H activation of alkynes. What's more, the *in situ* DRIFTS spectra clearly show the changes of alkyne substances in the catalytic process and the XPS results reveal the reduction and oxidation processes during the catalytic reaction, which are greatly helpful in proposing the mechanism of the homo-coupling of terminal alkynes. Further work is in progress in this laboratory with the aim of extending the application of the readily available synergistic Cu–POM catalytic systems in other coupling transformations and investigating the detailed mechanisms and intermediate structures.

Conflicts of interest

There are no conflicts to declare.

Acknowledgements

References

1. D. Ren, J. H. Fong and B. S. Yeo, The effects of currents and potentials on the selectivities of copper toward carbon dioxide electroreduction, *Nat. Commun.*, 2018, **9**, 8.
2. T. N. Huan, G. Rousse, S. Zanna, I. T. Lucas, X. Z. Xu, N. Menguy, V. Mougel and M. Fontecave, A Dendritic Nanostructured Copper Oxide Electrocatalyst for the Oxygen Evolution Reaction, *Angew. Chem., Int. Ed.*, 2017, **56**, 4792–4796.
3. B. H. Lee, S. Park, M. Kim, A. K. Sinha, S. C. Lee, E. Jung, W. J. Chang, K. S. Lee, J. H. Kim, S. P. Cho, H. Kim, K. T. Nam and T. Hyeon, Reversible and cooperative photoactivation of single-atom Cu/TiO_2 photocatalysts, *Nat. Mater.*, 2019, **18**, 620.
4. S. Kuld, M. Thorhauge, H. Falsig, C. F. Elkjaer, S. Helveg, I. Chorkendorff and J. Sehested, Quantifying the promotion of Cu catalysts by ZnO for methanol synthesis, *Science*, 2016, **352**, 969–974.
5. T. T. Zhuang, Z. Q. Liang, A. Seifitokaldani, Y. Li, P. De Luna, T. Burdyny, F. L. Che, F. Meng, Y. M. Min, R. Quintero-Bermudez, C. T. Dinh, Y. J. Pang, M. Zhong, B. Zhang, J. Li, P. N. Chen, H. Y. Liang, W. N. Ge, B. J. Ye, D. Sinton, S. H. Yu and E. H. Sargent, Steering post-C-C coupling selectivity enables high efficiency electroreduction of carbon dioxide to multi-carbon alcohols, *Nat. Catal.*, 2018, **1**, 421–428.
6. X. Zhou, C. G. Wang, Y. J. Zhang, F. Cheng, Y. He, Q. Shen, J. Shang, X. Shao, W. Ji, W. Chen, G. Q. Xu and K. Wu, Steering Surface Reaction Dynamics with a Self-Assembly Strategy: Ullmann Coupling on Metal Surfaces, *Angew. Chem., Int. Ed.*, 2017, **56**, 12852–12856.
7. W. R. H. Hurtley, CCXLIV.—Replacement of halogen in orthobromo-benzoic acid, *J. Chem. Soc.*, 1929, 1870–1873.

8. S. Bhunia, G. G. Pawar, S. V. Kumar, Y. W. Jiang and D. W. Ma, Selected Copper-Based Reactions for C-N, C-O, C-S, and C-C Bond Formation, *Angew. Chem., Int. Ed.*, 2017, **56**, 16136–16179.

9. D. W. Ma, Y. D. Zhang, J. C. Yao, S. H. Wu and F. G. Tao, Accelerating effect induced by the structure of alpha-amino acid in the copper-catalyzed coupling reaction of aryl halides with alpha-amino acids. Synthesis of benzolactam-V8, *J. Am. Chem. Soc.*, 1998, **120**, 12459–12467.

10. Q. A. Lo, D. Sale, D. C. Braddock and R. P. Davies, Mechanistic and Performance Studies on the Ligand-Promoted Ullmann Amination Reaction, *ACS Catal.*, 2018, **8**, 101–109.

11. E. Wang, K. Chen, Y. Chen, J. Zhang, X. Lin and M. Chen, Porous polymeric ligand promoted copper-catalyzed C-N coupling of (hetero)aryl chlorides under visible-light irradiation, *Sci. China: Chem.*, 2020, **64**, 17–21.

12. C. Sambiagio, S. P. Marsden, A. J. Blacker and P. C. McGowan, Copper catalysed Ullmann type chemistry: from mechanistic aspects to modern development, *Chem. Soc. Rev.*, 2014, **43**, 3525–3550.

13. G. Evano, N. Blanchard and M. Toumi, Copper-mediated coupling reactions and their applications in natural products and designed biomolecules synthesis, *Chem. Rev.*, 2008, **108**, 3054–3131.

14. S. V. Ley and A. W. Thomas, Modern synthetic methods for copper-mediated C(aryl) bond O, C(aryl) bond N, and C(aryl) bond S bond formation, *Angew. Chem., Int. Ed.*, 2003, **42**, 5400–5449.

15. J. S. P. Vogel, *"Copper(II) Acetate" in "EROS Encyclopedia of Reagents for Organic Synthesis" Copper(II) Acetate*, *John Wiley & Sons*, 2005.

16. B.-Q. Ma, K. L. Mulfort and J. T. Hupp, Microporous pillared paddle-wheel frameworks based on mixed-ligand coordination of zinc ions, *Inorg. Chem.*, 2005, **44**, 4912–4914.

17. S. A. Bourne, J. Lu, A. Mondal, B. Moulton and M. J. Zaworotko, Self-Assembly of Nanometer-Scale Secondary Building Units into an Undulating Two-Dimensional Network with Two Types of Hydrophobic Cavity, *Angew. Chem., Int. Ed.*, 2001, **40**, 2111–2113.

18. W. J. Cui, S. M. Zhang, Y. Y. Ma, Y. Wang, R. X. Miao and Z. G. Han, Polyoxometalate-Incorporated Metal-Organic Network as a Heterogeneous Catalyst for Selective Oxidation of Aryl Alkenes, *Inorg. Chem.*, 2022, **61**, 9421–9432.

19. X. Y. Yin, Y. Q. Zhang, Y. Y. Ma, J. Y. He, H. Song and Z. G. Han, Bifunctional Sensors Based on Phosphomolybdates for Detection of Inorganic Hexavalent Chromium and Organic Tetracycline, *Inorg. Chem.*, 2022, **61**, 13174–13183.

20. W. An, X. Zhang, J. Niu, Y. Ma and Z. Han, Unusual hexa-nuclear cadmium cluster functionalized phosphomolybdate as effective photoelectrochemical sensor for trace Cr(VI) detection, *Chin. Chem. Lett.*, 2022, **33**, 4400–4404.

21. D.-L. Long, E. Burkholder and L. Cronin, Polyoxometalate clusters, nanostructures and materials: from self assembly to designer materials and devices, *Chem. Soc. Rev.*, 2007, **36**, 105–121.

22. M. Nyman and P. C. Burns, A comprehensive comparison of transition-metal and actinyl polyoxometalates, *Chem. Soc. Rev.*, 2012, **41**, 7354–7367.

23. K. Kamata, S. Yamaguchi, M. Kotani, K. Yamaguchi and N. Mizuno, Efficient Oxidative Alkyne Homocoupling Catalyzed by a Monomeric Dicopper-Substituted Silicotungstate, *Angew. Chem., Int. Ed.*, 2008, **47**, 2407–2410.

24. C. H. Zhan, J. M. Cameron, D. Gabb, T. Boyd, R. S. Winter, L. Vila-Nadal, S. G. Mitchell, S. Glatzel, J. Breternitz, D. H. Gregory, D. L. Long, A. Macdonell and L. Cronin, A metamorphic inorganic framework that can be switched between eight single-crystalline states, *Nat. Commun.*, 2017, **8**, 7.

25. Z. G. Jiang, W. T. Mao, D. P. Huang, Y. Wang, X. J. Wang and C. H. Zhan, A nonconventional host-guest cubic assembly based on gamma-cyclodextrin and a Keggin-type polyoxometalate, *Nanoscale*, 2020, **12**, 10166–10171.
26. R. Bai, G. Zhang, H. Yi, Z. Huang, X. Qi, C. Liu, J. T. Miller, A. J. Kropf, E. E. Bunel, Y. Lan and A. Lei, Cu(II)-Cu(I) synergistic cooperation to lead the alkyne C-H activation, *J. Am. Chem. Soc.*, 2014, **136**, 16760–16763.
27. G. Zhang, H. Yi, G. Zhang, Y. Deng, R. Bai, H. Zhang, J. T. Miller, A. J. Kropf, E. E. Bunel and A. Lei, Direct observation of reduction of Cu(II) to Cu(I) by terminal alkynes, *J. Am. Chem. Soc.*, 2014, **136**(3), 924–926.
28. B. Zimmermann and G. Baranović, Two-dimensional infrared correlation spectroscopic study on thermal polymerization of diphenylbutadiyne, *Vib. Spectrosc*, 2006, **41**, 126–135.
29. T. H. Fleisch and G. J. Mains, An XPS study of the UV reduction and photochromism of MoO3 and WO3, *J. Chem. Phys.*, 1982, **76**, 780–786.
30. W. Feng, Y. Ding, Y. Liu and R. Lu, The photochromic process of polyoxometalate-based nanocomposite thin film by in situ AFM and spectroscopy, *Mater. Chem. Phys.*, 2006, **98**, 347–352.
31. B. L. Han, Z. Liu, L. Feng, Z. Wang, R. K. Gupta, C. M. Aikens, C. H. Tung and D. Sun, Polymorphism in Atomically Precise Cu-23 Nanocluster Incorporating Tetrahedral Cu-4 (0) Kernel, *J. Am. Chem. Soc.*, 2020, **142**(12), 5834–5841